J Mater Sci (2008) 43:696–701
DOI 10.1007/s10853-007-2188-3

Predicting porosity content in triaxial porcelain bodies as a function of raw materials contents

Sivaldo L. Correia · Dachamir Hotza · Ana M. Segadães

Received: 21 June 2007 / Accepted: 24 September 2007 / Published online: 31 October 2007

Abstract This work describes the relationships observed between the porosity of fired ceramic test pieces and the raw materials contents in the unfired mixture. The investigation was carried out using the mixture experiments design approach coupled with response surface methodology, which enables the calculation of statistically significant models for the properties from a limited number of experimental results. Ten formulations of a clay mixture, potash feldspar and quartz sand were processed in the laboratory under fixed conditions, similar to those used on wall and floor tile industrial practice, and characterized. Closed porosity (CP) was estimated from the analysis of back-scattered SEM photomicrographs, open porosity (OP) was calculated as the product of bulk density and water absorption, and total porosity (TP) was calculated from OP and CP values. Characterization results were used to calculate statistically significant and valid regression equations, relating those properties with the raw material contents in the unfired mixture. For the particular raw materials and processing conditions used, the models clearly show how quartz contributes to increasing OP and the crucial role played by feldspar when CP and TP are to be minimized (*circa* 3 vol.%), and how the clay content can counteract that effect and lead to maximum closed porosity (~14 vol.%).

S. L. Correia
Center of Technology Sciences (UDESC/CCT), State University of Santa Catarina, 89223-100 Joinville, SC, Brazil

D. Hotza
Department of Chemical Engineering (EQA), Federal University of Santa Catarina (UFSC), 88040-900 Florianopolis, SC, Brazil

A. M. Segadães (✉)
Department of Ceramics and Glass Engineering (CICECO), University of Aveiro, 3810-193 Aveiro, Portugal
e-mail: segadaes@ua.pt

Introduction

The response surface methodology, and the design of mixture experiments, is a collection of mathematical and statistical techniques that can be useful in the modelling, analysis and optimization of problems whose response is influenced by several variables [1, 2]. Certain properties of ceramic bodies and their dependence on the proportions of raw materials used in their fabrication rightfully fall within this scenario.

In porcelain and other traditional ceramics processing, the raw materials play one of three distinctive roles [3, 4]: plastic materials (generally clays), fluxing materials (usually feldspars) and inert materials or fillers (commonly quartz). The presence of those three types of raw materials determines many of the technological properties of industrial ceramics and explains the label "triaxial" generally used to designate such ceramic systems. This is why the response surface methodology can and has been used to model some of the technological properties of industrial ceramics as functions of those raw material contents [5–7].

Briefly, the methodology starts with a regular array of uniformly spaced points (simplex lattice), which is set on the composition triangle defined by the raw materials. Given the restrictions imposed by processing on clay, feldspar and quartz contents in the mixture of raw materials, only a sub-region of the original composition triangle is of interest and the concept of pseudo-component must be used to create a restricted composition triangle [2]. Then, the values of the property of interest are experimentally

determined on those selected lattice points. To better the confidence in the experimental results and guarantee their reproducibility, replications of the experiments are needed (i.e. the experimental procedure, from mixture preparation to characterization, has to be repeated for a number of times, for each simplex composition). A regression polynomial is then fitted to those experimental values and the model is considered valid only when the differences between the experimental and the calculated values (error) are uncorrelated and randomly distributed with a zero mean value and a common variance. A final validation of the model requires a couple of test compositions to countercheck the calculated statistical model. A more detailed description of the procedure can be found elsewhere [5–7].

After firing, wall and floor tile bodies are composed of glassy and crystalline phases and empty spaces (pores and fissures). Their volume and size distribution affect the industrial use of the material and its weathering behaviour. In particular, porosity is one of the technological properties of industrial ceramics of greater interest, as variations in porosity markedly affect the mechanical resistance and, hence, the final application of the materials [5–8].

The main objective of this work is to shed light on the relationship between the raw materials contents in the unfired mixture and the porosity of fired bodies, using digital image analysis techniques. To this aim, the design of mixture experiments methodology was used to mathematically model the closed, open and total porosities, as functions of the proportions of clay, feldspar and quartz present in the mixture of raw materials, under constant processing conditions. The models so obtained can be used to select the best combination of those three raw materials to produce a ceramic body with specified porosities.

Experimental

The raw materials used were potash feldspar, quartz sand and a clay mixture, all supplied by Colorminas (Criciúma, SC, Brazil). Details of the raw materials characterization can be found elsewhere [6].

These raw materials were located on a clay–feldspar–quartz composition triangle and a {3,2} centroid simplex-lattice design, augmented with interior points, was used to define the ten mixtures of those raw materials that should be investigated.

Mixtures with the selected compositions were wet processed, following the conventional porcelainized stoneware wall and floor tile industrial procedure: wet grinding (residue left in a 325 mesh sieve below 1 wt.%), drying (24 h), moisturizing (6.5 ± 0.2 wt.%, dry basis), granulation, uniaxial pressing at 47 MPa (Micropressa Gabbrielli, 10 ton hydraulic press), test piece drying (110 ± 5 °C until constant weight) and firing at 1,170 °C for 1 h (heating at 3.20 °C/min up to 600 °C, and at 4.75 °C/min from 600 to 1,170 °C), followed by natural cooling. For each composition, two independent batches were prepared and processed (replications).

The microstructure of the fired samples was studied on as-fracture surfaces by scanning electron microscopy (SEM, Philips XL 30, with an Energy Dispersion X-ray detector).

The water absorption was determined using Archimedes' liquid displacement method by immersion in boiling water for 2 h, on cylindrical test pieces (20×10 mm^3, 4.5 g of material per test piece), using a Denver DE 100A digital analytical scale with a resolution of 0.1 mg. For each mixture, the final test result was taken as the average of the measurements carried out on five test pieces.

The bulk density of fired test pieces was calculated geometrically, using the dimensions (1 μm resolution Mitutoyo MDC-25 M digital micrometer) and weight of cylindrical test pieces. It must be emphasized that not all the compositions can be regarded as true porcelain, hence a constant typical solid density of 2.65 g/cm^3 cannot be assumed. Instead of the usual measurement of the true solid density (e.g. He pycnometry) for every sample, a detailed microstructure study was preferred.

Closed porosity (CP) was calculated from back-scattered electron SEM images (Imago software, EMC, Federal University of Santa Catarina, Brazil) [9], the final result being the average of the measurements carried out on five images for each sample. Open porosity (OP) is the product of water absorption by bulk density and total porosity (TP) was calculated from OP and CP values.

The results of the two replications were used to iteratively calculate the coefficients of the regression equations, until statistically relevant models and response surfaces were obtained, relating the CP, OP and TP with the proportions of the clay, feldspar and quartz present in the unfired mixture. The calculations were carried out with Statistica 7.1 (StatSoft Inc., 2006).

Results and discussion

Characterization of raw materials and mixture compositions

The results of chemical composition (XRF) and the mineralogical constitution (XRD) of the clay mixture confirmed the presence of quartz (16 wt.%) and kaolinite (65 wt.%), muscovite (3 wt.%), montmorillonite (8 wt.%) and some potash feldspar (microcline, 7 wt.%). On the other hand, the quartz sand and the potash feldspar are rather pure materials (<0.5 wt.% impurities).

The raw materials can be represented in the triaxial composition triangle, as shown in Fig. 1: the quartz sand and the potash feldspar were considered to be pure and coincide with two of the triangle apexes, whereas the clay mixture must be divided into its clay mineral (plastic) fraction, feldspar fraction and quartz fraction (i.e. a point inside the composition triangle).

The chosen processing conditions require that lower bound composition limits are used, and those were 20 wt.% clay, 15 wt.% feldspar and 15 wt.% quartz. Thus, a restricted composition triangle of pseudo-components was created (also shown in Fig. 1), on which a {3,2} simplex lattice augmented with interior points was set. Figure 1 shows that the pseudo-components triangle lies inside the raw materials triangle, meaning that all ten simplex mixtures can be prepared.

The particle size distributions in all ten compositions were found to be very similar in all mixtures [7]. Thus, the effects of particle packing on porosity are expected to be the same for all compositions. Seventy-five percent of the particles are below 17 μm, which suggests high sinterability and optimizes the effect of quartz in the final sintered body [10–12].

Measured porosities and statistical analysis

Table 1 presents the porosity values obtained for the two replications of the ten mixtures. With the data shown in Table 1, regression equations were sought for each property, subjected to a significance level of 5%.

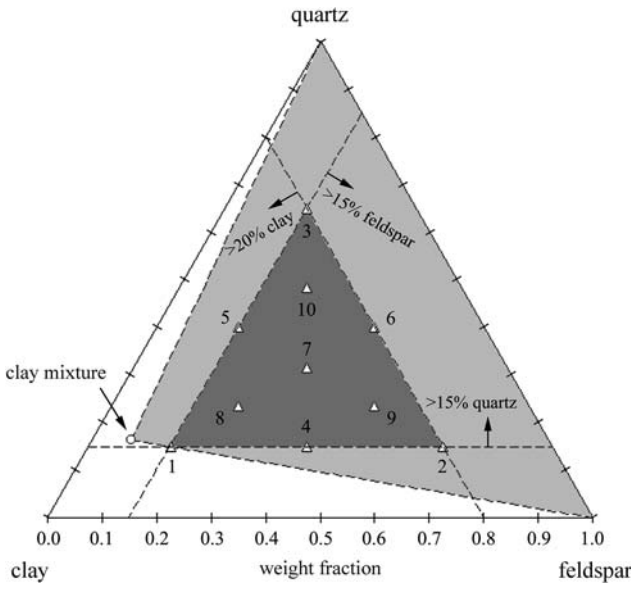

Fig. 1 The triaxial system clay–quartz–feldspar, showing the raw materials triangle (light grey), the restricted pseudo-components triangle (dark grey) and the simplex points (studied compositions)

Table 1 Values of CP, OP and TP obtained for the simplex mixtures in two replications

Mixture	OP (vol.%)	CP (vol.%)	TP (vol.%)
Replication 1			
1	0.61 ± 0.02	5.15 ± 0.65	5.76 ± 0.65
2	0.21 ± 0.01	7.51 ± 0.72	7.72 ± 0.72
3	23.57 ± 0.16	21.52 ± 1.18	45.09 ± 1.18
4	0.07 ± 0.01	8.72 ± 0.51	8.79 ± 0.51
5	7.32 ± 0.06	12.92 ± 0.50	20.24 ± 0.50
6	0.37 ± 0.04	8.44 ± 0.69	8.81 ± 0.69
7	0.50 ± 0.04	8.41 ± 0.71	8.91 ± 0.71
8	0.14 ± 0.01	13.57 ± 0.73	13.71 ± 0.73
9	0.14 ± 0.01	3.03 ± 0.47	3.17 ± 0.47
10	10.55 ± 0.20	10.94 ± 0.79	21.49 ± 0.79
Replication 2			
1	0.67 ± 0.03	5.79 ± 0.71	6.46 ± 0.71
2	0.09 ± 0.01	8.13 ± 0.73	8.22 ± 0.73
3	24.53 ± 0.16	23.70 ± 1.08	48.23 ± 1.08
4	0.10 ± 0.02	10.37 ± 0.74	10.47 ± 0.74
5	5.11 ± 0.05	13.54 ± 0.68	18.65 ± 0.68
6	0.28 ± 0.03	9.66 ± 0.67	9.94 ± 0.67
7	0.58 ± 0.03	8.46 ± 0.73	9.04 ± 0.73
8	0.10 ± 0.01	12.77 ± 0.64	12.87 ± 0.64
9	0.14 ± 0.01	3.21 ± 0.51	3.35 ± 0.51
10	9.93 ± 0.24	10.29 ± 0.53	20.22 ± 0.53

Table 2 shows the results of the variance analysis for the best regressions obtained for OP, CP and TP (major statistical properties: p-value, coefficient of multiple determination R^2, and adjusted coefficient of multiple determination, R^2_A), using the nomenclature commonly found in the literature [1, 2]. It can be seen that all models are statistically significant at the required level (p-value ≤ significance level) and present small variability (high coefficients of multiple determination).

Table 2 also presents the results of lack-of-fit tests, used to check the adequacy of the models [1, 2]. In these tests, the p-value exceeds the significance level, meaning that the models do not display lack of fit. In all cases, the errors could be considered randomly distributed around a zero mean value (i.e. are uncorrelated), which suggests a

Table 2 Major statistical properties, relevant for variance analysis and lack-of-fit tests

Model	Variance analysis results		Lack-of-fit results	
	p-value	R^2	R^2_A	p-value
OP, full cubic	0.0474	0.9898	0.9850	0.0756
CP, full cubic	0.0000	0.9854	0.9747	0.0935
TP, full cubic	0.0001	0.9964	0.9939	0.5608

common constant variance. On the basis of this analysis, the full cubic regressions obtained were accepted to describe the effect of raw materials in OP, CP and TP.

Effect of the mixture composition on porosities

The Pareto chart of effects is an effective tool for communicating the results of an experiment. In such graph, the variance analysis effect estimates are sorted from the largest absolute value to the smallest absolute value. A horizontal bar represents the magnitude of each effect and, often, a vertical line going across the bars indicates how large an effect has to be (i.e. how long a bar must be) to be statistically significant.

Figure 2a shows the Pareto chart of effects for OP. The chart indicates that there are four statistically significant factors, which clearly have a much larger effect than the others and must be the OP controlling factors: the quartz content (x_3), the quartz–feldspar content interaction (x_2x_3), the clay–quartz content interaction (x_1x_3) and the feldspar (x_2) content. The quartz content (x_3) and the feldspar content (x_2) affect the property in an antagonistic manner (in Fig. 2a, positive magnitude of 24.08 and 4.26, respectively), i.e. quartz and feldspar contribute to the increase of OP. In fact, Fig. 2b shows that the maximum of OP is achieved with high contents of quartz, while increasing feldspar contents lead to more modest increases in OP.

The main synergistic interactions observed in Fig. 2a, for decreasing OP, are those observed between the feldspar and quartz contents (x_2x_3) and the clay and quartz contents (x_1x_3), which show negative magnitudes of 14.10 and 7.14, respectively. This phenomenon is presumably linked to a partial opening of some closed pores and/or to the occurrence of micro-cracks, rather than excessive vitrification, resulting in bloating [8, 13].

As for the effect of increasing clay contents (x_1), Fig. 2a suggests a mild influence on the open porosity, rendered quite evident on Fig. 2b. Figure 2b also shows that there is a rather forgiving composition range of medium-to-high feldspar and clay contents (above 35–40 wt.%), in which OP is determined almost solely by the quartz content.

Figure 3a shows the Pareto chart of effects for CP, which indicates that there are seven statistically significant

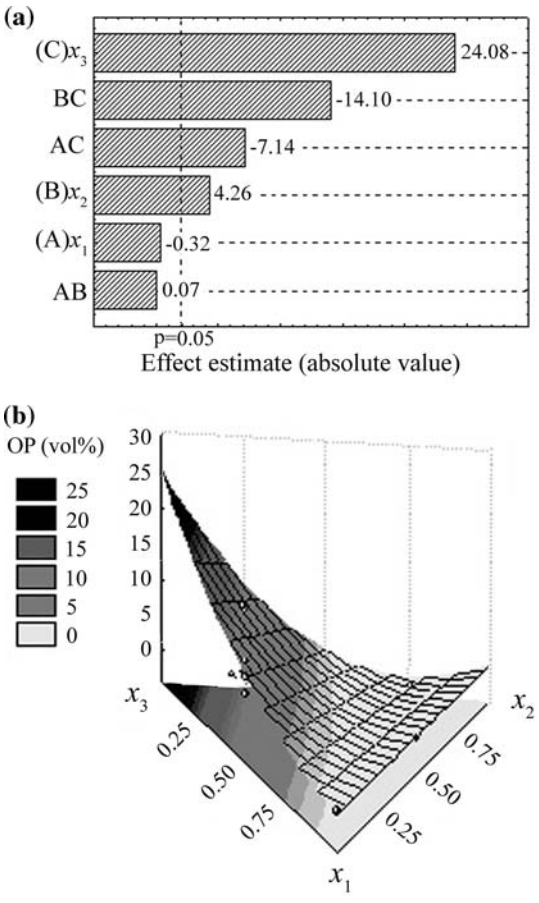

Fig. 2 (**a**) Pareto chart of standardized effects for OP; (**b**) Predicted open porosity surface (OP) as a function of composition

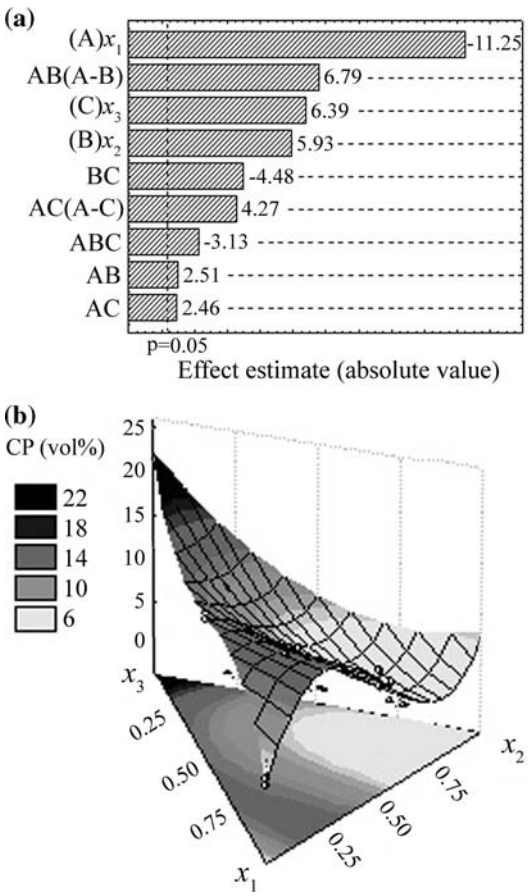

Fig. 3 (**a**) Pareto chart of standardized effects for CP; (**b**) Predicted closed porosity surface (CP) as a function of composition

factors that, clearly, have a much larger effect than the others. The clay content (x_1), the feldspar–quartz content interaction (x_2x_3) and the clay–feldspar–quartz content interaction ($x_1x_2x_3$) are the main controlling factors for decreasing CP (in Fig. 3a, negative magnitude of 11.25, 4.48 and 3.13, respectively). This fact is well demonstrated in Fig. 3b, by the complicated evolutions of the CP response surface.

Figure 3b shows that closed porosity behaves very differently from open porosity. Again, decreasing quartz content leads to denser bodies and its effect on CP is similar to that on OP. However, the effects of clay and feldspar on CP are very different from those on OP.

Clearly, there is an optimum feldspar content (~50 wt.%) that minimizes the closed porosity (~3 vol.%), and the very worst clay content, leading to maximum closed porosity (~14 vol.%), lies at ~55 wt.%. For higher clay contents, the closed porosity diminishes, probably due to the amount of micaceous and montmorillonitic minerals in the clay mixture, which contribute to a lower liquid phase viscosity and, hence, easier flow into pores [13, 14].

Figure 4 illustrates the differences in pore morphology, as seen on fracture surfaces by SEM, and shows that the raw materials also affect closed pore characteristics and the microstructure (see Fig. 1 for composition location).

Upon firing, composition 1 (Fig. 4a) mostly contains isolated and irregular elongated pores (average 5.47 vol.% CP, Table 1) in the diameter range 1–20 μm. Such pore morphology can be due to a higher liquid phase viscosity caused by the low feldspar content, despite the high clay content [15].

The fired composition 2, Fig. 4b, with an average CP value of 7.82 (Table 1), is characterized by isolated, spherical, small pores (1–15 μm).

In contrast, compositions 3 and 5 (Fig. 4c and d, respectively) are clearly not well-sintered, as they are characterized by a larger amount of interconnected irregularly shaped pores in the size range of 10–30 and 5–20 μm, respectively.

Figure 5 shows the effect of raw materials on the total porosity (TP). Given that CP is much higher than OP in all but composition 3, the TP surface generally follows the trends shown by the CP surface in Fig. 3b.

Again, there is an optimum feldspar content that minimizes the total porosity and a worst clay content that leads to high TP. The minimum TP (~3 vol.%) corresponds to ~50 wt.% feldspar, the proportion between clay and quartz being slightly above unity. Clay contents above ~55 wt.% (and equal contents of the other two components) again contribute to decrease the total porosity.

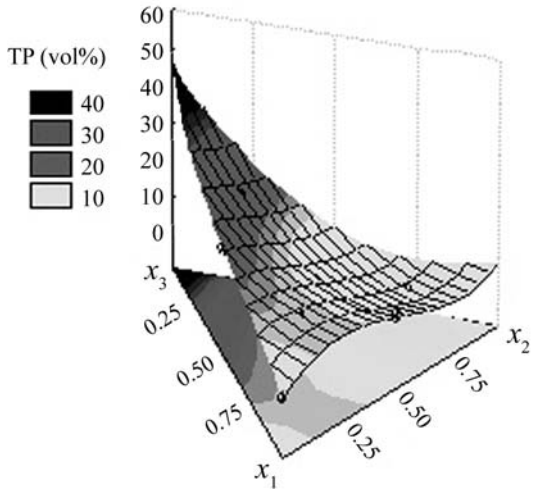

Fig. 5 Predicted total porosity surface (TP) as a function of composition

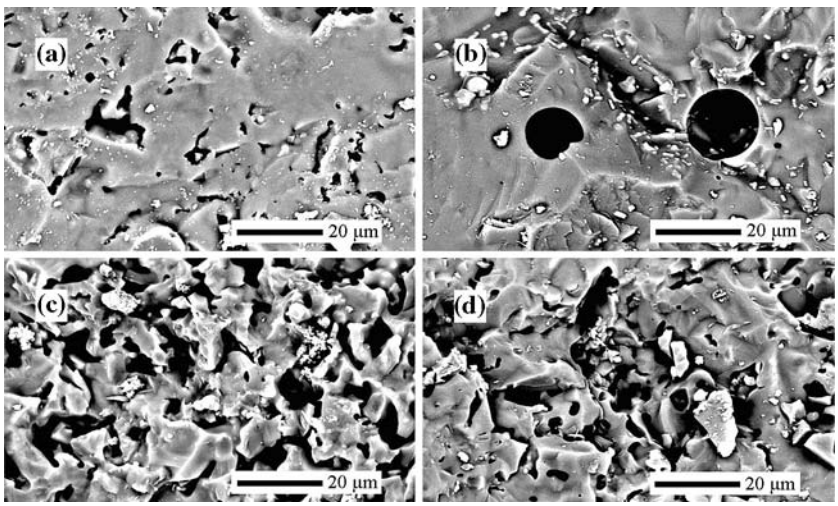

Fig. 4 SEM photographs of as-fractured surfaces of fired samples, showing the pore characteristics in compositions (see Fig. 1 for composition location): (**a**) 1; (**b**) 2; (**c**) 3; and (**d**) 5

Conclusions

The methodology of mixtures design proved to be a useful tool for planning and analysing experiments on the influence of raw materials on open, closed and total porosities of ceramic triaxial bodies. The calculated regression models were found to be statistically significant at the required level and presented small variability.

For the particular raw materials and processing conditions used, the results obtained show that there is a rather forgiving composition range of medium-to-high feldspar and clay contents (above 35–40 wt.%), in which open porosity is determined almost solely by the quartz content and increases with it.

On the contrary, there is an optimum feldspar content ($\sim$50 wt.%) that minimizes closed porosity, and the very worst clay content, leading to maximum closed porosity ($\sim$14 vol.%), lies around 55 wt.% clay.

Given that closed porosity is generally much higher that open porosity, the total porosity tends to follow the trends shown by closed porosity.

Acknowledgements The authors appreciate the financial support received from the Brazilian Research Agency CAPES in the form of a Ph.D. grant (S.L. Correia), and are thankful to Colorminas for providing the raw materials used throughout the work.

References

1. Myers RH, Montgomery DC (2002) Response surface methodology: process and product optimization using designed experiments. John Wiley & Sons, New York
2. Cornell JA (2002) Experiments with mixtures: designs, models and the analysis of mixture data, 3rd edn. John Wiley & Sons
3. Reed JS (1998) Introduction to the principles of ceramics processing, 2nd edn. John Wiley & Sons, p 395
4. Amoros Albaro JL, Blasco Fuentes A, Enrique Navarro JE, Negre Medall F, Manfredini T, Pozzi P (1990) Ind Ceram 10:73
5. Correia SL, Curto KAS, Hotza D, Segadães AM (2004) J Eur Ceram Soc 24:2813
6. Correia SL, Hotza D, Segadães AM (2005) CFI—Ceram Forum Int 82:E39
7. Correia SL, Novaes APN, Hotza D, Segadães AM (2006) J Am Ceram Soc 89:3356
8. Carty WM, Senapati U (1998) J Am Ceram Soc 81:3
9. Appoloni CR, Fernandes CP, Innocentin MDM, Macedo A (2004) Mater Res 7:557
10. Manfredini T, Pellacani GC, Romagnoli M (1995) Am Ceram Soc Bull 74:76
11. Ece OI, Nakagawa ZE (2002) Ceram Int 28:131
12. Stathis G, Ekonomakou A, Stournaras CJ, Ftikos C (2004) J Eur Ceram Soc 24:2357
13. Khalfaoui A, Kacim S, Hajjaji M (2006) J Eur Ceram Soc 26:161
14. Maiti KN, Kumar S (1992) Ceram Int 18:403
15. Tucci A, Esposito L, Rastelli E, Palmonari C, Rambaldi E (2004) J Eur Ceram Soc 24:83